Microbial Cell Factories

RESEARCH

Open Access

A CRISPR-Cas9 system for knock-out and knock-in of high molecular weight DNA enables module-swapping of the pikromycin synthase in its native host

Zhe-Chong Wang[1], Hayden Stegall[1], Takeshi Miyazawa[1] and Adrian T. Keatinge-Clay[1*]

Abstract

Background Engineers seeking to generate natural product analogs through altering modular polyketide synthases (PKSs) face significant challenges when genomically editing large stretches of DNA.

Results We describe a CRISPR-Cas9 system that was employed to reprogram the PKS in *Streptomyces venezuelae* ATCC 15439 that helps biosynthesize the macrolide antibiotic pikromycin. We first demonstrate its precise editing ability by generating strains that lack megasynthase genes *pikAI-pikAIV* or the entire pikromycin biosynthetic gene cluster but produce pikromycin upon complementation. We then employ it to replace 4.4-kb modules in the pikromycin synthase with those of other synthases to yield two new macrolide antibiotics with activities similar to pikromycin.

Conclusion Our gene-editing tool has enabled the efficient replacement of extensive and repetitive DNA regions within streptomycetes.

Keywords Pikromycin, Type I PKSs, CRISPR/Cas9, Riboswitch, Updated module boundary, Module-swapping, PKS engineering, *S. venezuelae* ATCC 15439

Background

The genus of bacteria, *Streptomyces*, is well known for its remarkable ability to produce diverse bioactive metabolites[1]. Among these are the macrolide antibiotics, whose carbon skeletons are biosynthesized by modular polyketide synthases (PKSs) (Fig. 1)[2–4]. These enzymatic assembly lines are comprised of modules, each of which minimally consists of three functional domains: an acyltransferase (AT) that selects an α-carboxyacyl extender unit, an acyl carrier protein (ACP) that fuses the extender unit to a polyketide intermediate bound to the upstream module, and a ketosynthase (KS) that acquires the acyl chain and fuses it with an extender unit bound to the downstream module. A module may also contain processing domains, such as a ketoreductase (KR), dehydratase (DH), and enoylreductase (ER), that modify the elongated polyketide intermediate [5–7]. The traditional definition of a module, with KS at the upstream position, has guided module-swapping for three decades [8, 9]. However, recent studies have revealed that processing domains evolutionarily comigrate with the downstream KS and that native ACP/KS interfaces should be preserved when engineering PKSs [10–15]. Indeed, module-swapping using the updated module boundary, with KS at the downstream position, has been observed to consistently outperform module-swapping using the traditional boundary [14–16].

*Correspondence:
Adrian T. Keatinge-Clay
adriankc@utexas.edu
[1] Department of Molecular Biosciences, The University of Texas at Austin, Austin, TX 78712, USA

CRISPR-Cas9 (clustered regularly interspaced short palindromic repeats and CRISPR-associated protein 9) allows customizable edits to genomic DNA. It consists of a Cas9 endonuclease and a single-guide RNA (sgRNA). Cas9 navigates to the genomic locus specified by the sgRNA and generates a double-strand DNA break (DSB). This DSB can be imprecisely repaired by the non-homologous end-joining (NHEJ) [17]. Alternatively, it can be precisely repaired through homologous recombination if a DNA donor template is available, as in homology directed repair (HDR). Since DSBs are cytotoxic and limit the efficiency of precise gene modification, researchers have developed various strategies including tuning Cas9 expression, base editing, and prime editing [18–20]. Additionally, paired-guide prime editing techniques aim to facilitate the insertion of up to 5 kb [21, 22]. Although these innovative approaches have made significant strides, current genome-editing methods still face challenges inserting or replacing large DNA segments at specific genome loci with high efficiency. Cas9 expression can be tuned using riboswitches, regulatory RNA elements found across a wide range of organisms [23, 24]. Riboswitches undergo conformational changes upon binding to small molecule ligands and can regulate gene expression [25–27]. Theophylline-responsive riboswitches can regulate gene expression in *Streptomyces* and are valuable tools due to their high specificity, simple and reversible control, minimal genetic engineering, and low basal activity [28–30].

Pikromycin (**1**) is a 14-membered macrolide antibiotic whose carbon skeleton is biosynthesized by a prototypical, modular PKS (*pikAI-pikAIV*) in *Streptomyces venezuelae* ATCC 15439. Its structure is similar to the semisynthetic ketolide antibiotics that show activity against respiratory pathogens resistant to traditional antibiotics [31]. This resemblance has triggered researchers to generate pikromycin derivatives through combinatorial biosynthesis [32–35]. However, because the modular PKSs of *Streptomyces* are encoded by lengthy genes with high GC content, the efficacy of conventional cloning techniques is significantly hampered. To overcome this, various in vitro and in vivo CRISPR-Cas9 editing systems as well as allelic exchange methodologies have been developed [36–39]. However, the in vivo approaches still face challenges, including the cytotoxicity of Cas9, low efficiency of homologous recombination, and the low success rates of editing extensive DNA regions. Riboswitches have improved genome editing efficiency in *Streptomyces* through reducing the cytotoxic effects associated with Cas9 expression; however, their application is still limited to gene deletion [40]. Recently, pKCcas9dO CRISPR-Cas9 was developed and used to both delete cytochrome P450 and ferredoxin genes (~ 200–2000 bp) as well as insert *kasO*p* (~ 100 bp) into the genome of *S. venezuelae* ATCC 15439; however, chromosomal instability during this editing caused the loss of a large genomic region (0.6 Mbp, 6.7% of the genome), inversion and translocation of a large DNA segment, additional copy of a genome fragment, and unexpected loss of genes [41, 42].

In this study, a CRISPR-Cas9-based system was designed to efficiently edit extensive DNA regions within the pikromycin biosynthetic gene cluster of *S. venezuelae*. This system employs a constitutive *ermE** promoter and a modified theophylline-inducible riboswitch E* to co-regulate the expression of Cas9. This enhances transformation efficiency by mitigating the cytotoxicity associated with Cas9 while still exerting robust genetic-editing capabilities upon induction. The system also includes the segregationally-unstable pIJ101 replicon to help prevent undesirable genetic rearrangements often encountered when editing the repetitive genes of modular PKSs [43]. Using this CRISPR-Cas9 system, we demonstrate the ability to precisely delete or replace large DNA fragments. Seamless, in vivo module-swapping was performed within *S. venezuelae* to yield two new pikromycin derivatives that were characterized by NMR and are nearly as active against *Bacillus subtilis* as pikromycin.

(See figure on next page.)

Fig. 1 Module-swapping of the pikromycin PKS. **A** The 7 modules of the pikromycin PKS (**P1**-**P7**, updated boundaries), are housed by the 4 polypeptides encoded by *pikAI-pikAIV*. A heptaketide intermediate is cyclized into the 14-membered macrolactone narbonolide by the thioesterase (TE) domain. Narbonolide is desosaminylated by DesVII/DesVIII, and narbomycin (**2**) is hydroxylated by PikC to pikromycin (**1**). **B** The 6th module of the pikromycin PKS was replaced by the 6th module of the erythromycin PKS, and the **P6**/**E6**-swapped strain, ZC1, generated pikromycin (**1**). **C** The 2nd module of the pikromycin PKS was replaced by the 2nd module of the tylosin PKS, and **P2**/**T2**-swapped strain, ZC2, generated narbomycin derivative **3**. **D** The 1st module of the pikromycin PKS was replaced by the 1st module of the venediol PKS, and the **P1**/**V2**-swapped strain, ZC3, generated narbomycin derivative **4**. Circles, hexagons, stars, and squares represent PKS domains. Docking domains are shown as wedged ends. ACP, acyl carrier protein; KS, ketoacyl synthase; KS^{Q}, KS-like decarboxylase; AT, acyltransferase; KR, ketoreductase; KR^{0}, KR-like epimerase; DH, dehydratase; ER, enoylreductase; DesVII/DesVIII, the desosaminyltransferase; PikC, cytochrome P450 hydroxylase; **E6**, module 6 of erythromycin PKS; **T2**, module 2 of tylosin PKS; **V1**, module 1 of venediol PKS. The structural changes of derivatives introduced by module-swapping are marked with dashed red circles

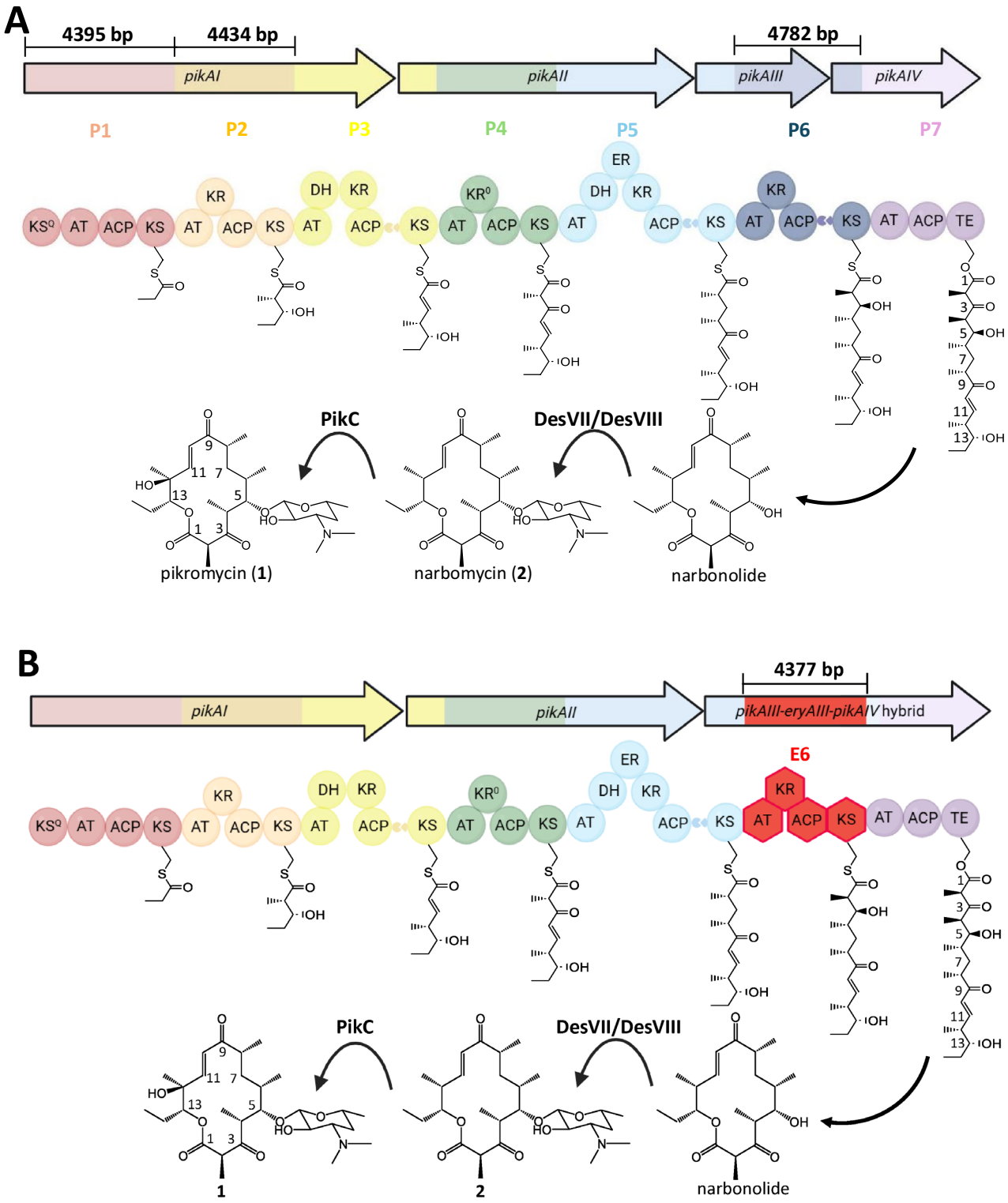

Fig. 1 (See legend on previous page.)

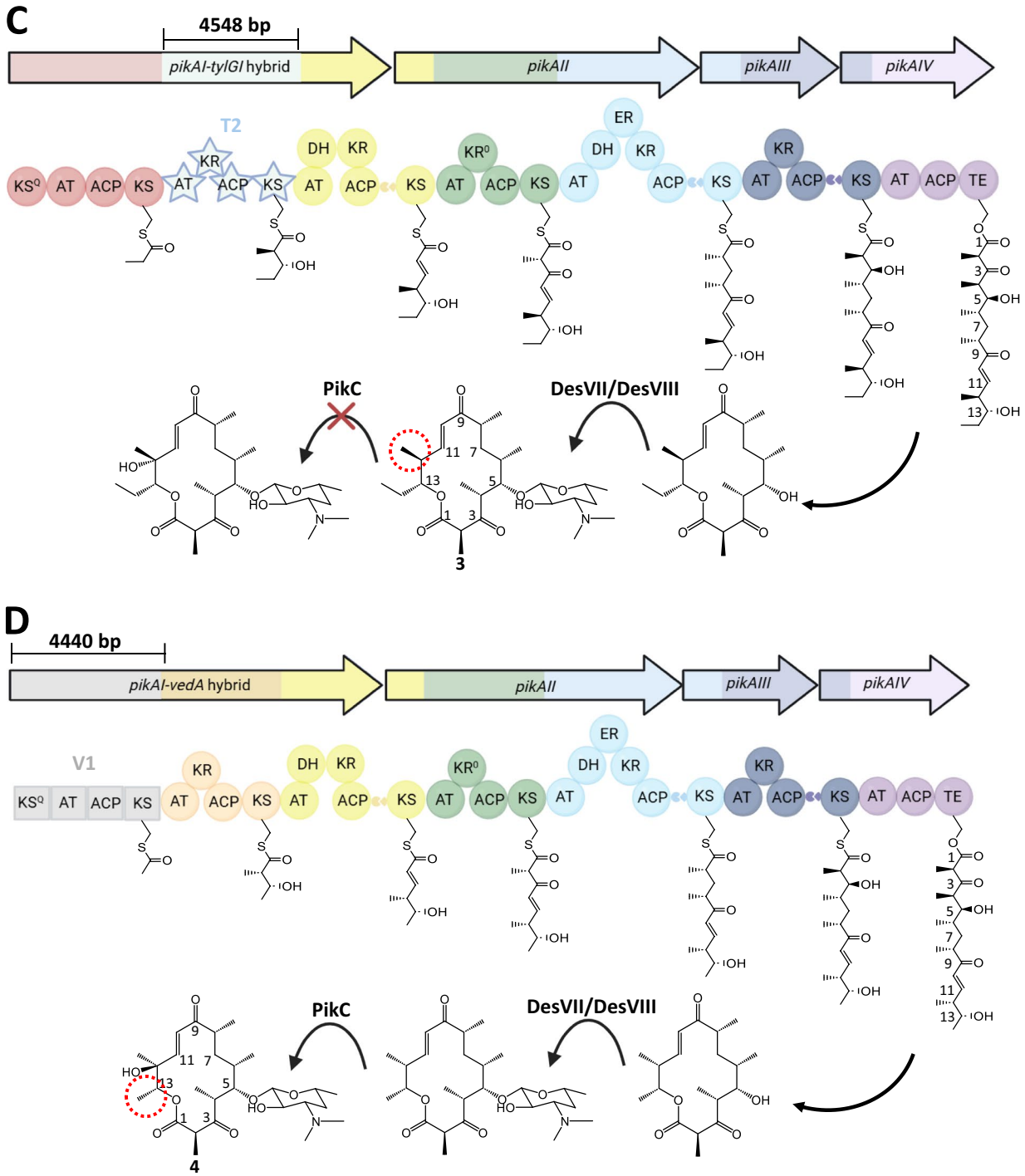

Fig. 1 continued

Methods

Bacterial strains, plasmids, and media

The bacterial strains and plasmids utilized in this research are described (Additioanl file 1: Table S1). *Escherichia coli* DH5α competent cells were employed for standard cloning procedures. *S. venezuelae* ATCC 15439 served as the host strain for the engineering and expression of the hybrid pikromycin derivatives. *B. subtilis* strain 168 was utilized for the microbial susceptibility assessment. *E. coli* cultures were maintained at 37 °C

on LB agar plates or broths containing the appropriate antibiotics, with liquid cultures incubated on a shaker platform at 200 rpm. Various media, including mannitol soya flour (MS) agar (20 g/L mannitol, 20 g/L soya flour, 20 g/L agar), R5 regeneration medium agar (22 g/L agar, 103 g/L sucrose, 0.25 g/L K_2SO_4, 10.12 g/L $MgCl_2{\cdot}6H_2O$, 10 g/L glucose, 0.1 g/L casamino acid, 5 g/L yeast powder, 5.73 g/L TES, 0.005% KH_2PO_4, 0.02 M $CaCl_2$, 0.3% L-proline, 0.007 N NaOH, and 0.002% trace element solution), SPA medium agar (1 g/L yeast extract, 1 g/L beef extract, 2 g/L tryptone, 10 g/L glucose, trace amount of $FeSO_4$, and 15 g/L agar), AS-1 agar (1 g/L yeast extract, 5 g/L soluble starch, 0.2 g/L L-alanine, 0.2 g/L L-arginine, 0.5 g/L L-asparagine, 2.5 g/L NaCl, 10 g/L Na_2SO_4, and 20 g/L agar), TSB medium agar (17 g/L tryptone, 3 g/L soytone, 2.5 g/L dextrose, 5 g/L NaCl, 2.5 g/L K_2HPO_4, 15 g/L agar) and fermentation medium (10 g/L glucose, 10 g/L glycerol, 10 g/L polypeptone, 5 g/L meat extract, 5 g/L NaCl, 2 g/L $CaCl_2$, 1 g/L yeast extract) [32, 44–46], were used to support the growth and production of pikromycin derivatives. Antibiotics used included apramycin (50 μg/mL), kanamycin (50 μg/mL), chloramphenicol (35 μg/mL), and nalidixic acid (25 μg/mL).

Construction of non-targeting CRISPR/Cas9 plasmids

In this study, we engineered seven distinct CRISPR-Cas9 expression systems, designated as pMKR02 through pMKR08, through a multistep fabrication process. Initially, we PCR-amplified a DNA fragment, which contained the *Streptomyces*-optimized *cas9* gene, guide RNA scaffold, apramycin resistance gene, and ColE1 origin of replication, from the pCRISPomyces-2 plasmid using primer set P1/P2 (Additioanl file 1: Table S2) [47]. This amplified segment was then integrated into the wzc05 plasmid using NdeI and XbaI restriction sites, generating an intermediate construct termed wzc-*cas9* [48]. Subsequently, we further PCR-amplified a DNA fragment from the wzc-*cas9* plasmid using primer set P3/P4 and assembled it with two additional components: the RK2 conjugal transfer origin and the pIJ101 replicon segment, which were amplified using primer sets P5/P6 and P7/P8 individually from pYH7, through Gibson assembly (New England Biolabs, E2611S), resulting in the CRISPR-Cas9 system, pMKR08 [49]. To develop the theophylline-inducible variants, pMKR02-07, we first synthesized the riboswitch DNA elements by annealing complementary primer sets, P9/P10, P11/P12, P13/P14, P15/P16, P17/P18, and P19/P20 respectively, and then fused them with DNA fragments amplified from pMKR08 using primer sets P21/P22 and P23/P24 via Gibson assembly. Additionally, for analyzing the transformation efficiency of these CRISPR/Cas9 systems, we constructed pMKR01 plasmid, which contains most DNA fragment of pMKR08 except the region of *ermE** promoter and *cas9* gene, by NdeI-digestion and self-ligation of the DNA fragments amplified from pMKR08 with primer set P25/P26. The accuracy of these constructs, pMKR01-pMKR08, was validated through comprehensive whole plasmid sequencing performed by Plasmidsaurus.

Construction of specific gene-targeting CRISPR/Cas9 plasmids

The targeting constructs were generated through a combination of Golden Gate assembly and traditional restriction enzyme-based cloning. Specifically, the CRISPR-Cas9 spacer inserts were produced by annealing pairs of 24-base oligonucleotides, which were then individually integrated into the CRISPR-Cas9 plasmids via Golden Gate assembly with the BbsI enzyme. To ensure the specificity of Cas9 and minimize off-target activity, the target sites were carefully chosen. The terminal 12 nucleotides of the protospacer, along with the protospacer adjacent motif (PAM), which are known as the "seed sequence", play a critical role in determining Cas9 specificity. Therefore, we selected target sites that were unique within the genome for the terminal 12 nucleotides of the protospacer and the PAM. This was confirmed through BLAST analysis against the genomic sequence (GenBank Accession Number: CP013129) [47, 50, 51]. To create CRISPR-Cas9 plasmids containing dual spacer inserts, two individual plasmids were first constructed, each with a unique spacer. The second spacer was then amplified from one of these plasmids using the P27/P28 primer set, digested with XbaI and SpeI, and inserted into the XbaI site of the other CRISPR-Cas9 plasmid. For deleting DNA fragments through HDR, editing templates with 1.5 kb homology arms were amplified from *S. venezuelae* genome and integrated into the XbaI-digested CRISPR-Cas9-derived plasmids carrying the corresponding spacer inserts. Similarly, to swap variant modules into PKS genes, the target DNA segments were amplified from the organism's genome, fused with 1.5 kb repair arms using extension PCR, and then inserted into pMKR07-derived plasmids harboring spacer inserts via XbaI/SpeI digestion and ligation. The correct assembly of all plasmids was verified through restriction enzyme diagnostic digestion and whole plasmid sequencing.

Transformation efficiency assay

To investigate the impact of the CRISPR/Cas9 system on the transformation efficiency of *S. venezuelae* ATCC 15439, a mixture of the strain's protoplasts and 100 ng of CRISPR/Cas9 DNA was plated in triplicate using a 1:10 serial dilution. The total number of transformants harboring diverse CRISPR/Cas9 systems was estimated at the same dilution level, with the results presented as the

mean ± standard deviation from three independent transformation experiments.

Genetic manipulation of *S. venezuelae* ATCC15439

The preparation of protoplasts and transformation of *S. venezuelae* ATCC 15439 were performed using established protocols [44]. After transformation, individual colonies harboring CRISPR-Cas9 derivative plasmids for genetic modification were randomly selected, re-streaked onto SPA agar plates supplemented with apramycin and 4 mM theophylline, and incubated at 28 °C for 3–5 days. These CRISPR-Cas9 engineered bacterial colonies were then analyzed via PCR targeting the genomic region of interest. Colonies exhibiting the desired genetic modifications were plated on antibiotic-free MS agar at 28 °C for 3–5 days to facilitate plasmid clearance. The spores were serially diluted and plated on antibiotic-free SPA agar at 28 °C for 3 days. Single colonies were re-streaked onto SPA agar plates supplemented with or without apramycin to confirm the plasmid clearance, and the mutants of interest were further verified through PCR amplification, identifying the sequence of amplicons using specific primers by Sanger sequencing, or whole-genome sequencing by Plasmidsaurus (Additioanl file 1: Fig. S1).

Semiquantitative analysis of GusA activities directly on plates

To investigate the impacts of riboswitch E* and modified riboswitch E* on the expression level of the downstream gene, we amplified the DNA fragment from pMKR06 and pMKR07 with P110/P111 and P112/P111 respectively, and fused them with the *gusA* gene, which was amplified from pGMGUS (addgene #115678) with primer sets P113/P114 and P115/P114 individually, through Gibson assembly. The resultant reporter plasmids, pE*-Gus and pmE*-Gus plasmids were introduced into *S. venezuelae* by protoplast-mediated transformation, and the transformants were cultured on SPA medium agar plate supplemented with apramycin and theophylline. After 1, 2, and 3 days of incubation, each plate was overlaid with 2 mL of 40 mM 5-bromo-4-chloro-3-indolyl-beta-D-glucuronic acid (X-gluc) solution for visualization of GusA activity [52].

Construction of complementary plasmids

To further validate the precise editing capabilities of the pMKR07 system, we generated a series of complementary plasmids for heterologous expression. Employing previously reported methodology [53], we amplified DNA fragments containing partial regions of *pikAI*, *pikAII*, *desVIII*, and *desR* utilizing specific primer sets. These fragments were then individually cloned into the wzc02 or pMKBAC02 BAC vectors. Subsequently, we utilized protoplast-mediated transformation to integrate these plasmids into the chromosomal DNA of *S. venezuelae* via homologous recombination. The genomic DNA of the transformants was then prepared, digested, and self-ligated. The ligation mixture was transformed into 10G BAC-optimized electrocompetent cells, and the recombinants were selected on apramycin-containing LB-agar. Next, the resulting plasmids were further analyzed to ensure proper construction through whole plasmid sequencing, and the attP-intΦC31 DNA fragments were inserted. The wzc02-derived plasmid containing the *pikAI* gene was named W1, and the pMKBAC02 derived BAC carrying the whole pikromycin PKS cluster was denoted as BP. Finally, we inserted the *pikAI* promoter region amplified from the *S. venezuelae* genome into the plasmids that respectively contain the *pikAII* and *pikAIII-desVIII* regions to drive the expression of downstream genes, and the resultant plasmids were named W2 and W3.

Production, isolation, and analysis of compounds

The strains were cultured for 48 h in fermentation medium at 250 rpm and 28 °C. Following centrifugation, the broth was extracted twice with ethyl acetate and analyzed using LC/HRMS [6230 TOF LC/MS equipped with a ZORBAX RRHD Eclipse Plus C18 Column (2.1 × 50 mm) with a flow rate of 0.2 mL min^{-1} (solvent A, water with 0.1% formic acid; solvent B, acetonitrile with 0.1% formic acid. 2–100% B for 10 min, 100% B for 2 min), positive mode]. The extract was then separated using a silica gel column. Purified compounds were dissolved in methanol and injected onto an Agilent 6230 TOF LC/MS system connected to a CAPCELL PAK MGIII C18 column (250 mm × 4.6 mm, 5 μm) (Osaka Soda), which was equilibrated with 20% acetonitrile and 0.1% formic acid. Elution was performed using a gradient from 20 to 50% acetonitrile for 20 min at a flow rate of 1 mL/min, and the compounds were observed at 225 nm and collected.

NMR experiments

NMR spectroscopy was conducted using Varian Direct-Drive spectrometers at the NMR Facility in the Chemistry Department at the University of Texas at Austin. ^{13}C NMR spectra were acquired with proton broadband decoupling. Deuterated solvents served as internal references for the NMR measurements, and chemical shifts are reported in parts per million (ppm) relative to $CDCl_3$, with ^{1}H NMR referenced to 7.26 ppm and ^{13}C NMR referenced to 77.16 ppm.

Chiral chromatography

Purified compounds were dissolved in methanol and injected onto an Agilent 6230 TOF LC/MS connected to a CHIRALPAK®IF-3 Column (Daicel) (4.6×250 mm) equilibrated with 25% acetonitrile and 0.1% formic acid. Elution was performed through isocratic flow with the same solvent system. Compounds were observed at 225 nm and by ion count.

MIC assay

The antibacterial activities of **1**–**4** were evaluated against *B. subtilis* strain 168 according to the Clinical and Laboratory Standards Institute (CLSI) broth microdilution method. Freshly cultured *B. subtilis* cells in Mueller–Hinton medium were diluted 1:500 and used as the inoculum. After incubating the cells for 24 h at 37 °C in the presence of two-fold serial dilutions of the compounds, the minimum inhibitory concentration (MIC) was determined as the lowest concentration that prevented visible bacterial growth in the wells.

Results

Impact of riboswitches on the transformation efficiencies of CRISPR-Cas9 systems

To minimize unintended DNA recombination associated with the widely-used, temperature-sensitive pSG5 replicon in CRISPR-Cas9 tools for *Streptomyces*, we selected the segregationally-unstable pIJ101 replicon [54, 55]. As this replicon has been successfully utilized in the design of CRISPR-Cas9 tools for deleting highly-repetitive DNA sequences, pIJ101 was incorporated into the construction of our initial CRISPR-Cas9 plasmid, pMKR08 [43]. The constitutive *ermE** promoter was also utilized to access the Cas9 levels required for effective genome editing. To screen for an appropriate theophylline-responsive riboswitch, versions A, B, C, D, and E* were integrated into pMKR08, yielding pMKR02-pMKR06 (Additioanl file 1: Fig. S2 and Table S3) [56, 57]. Moreover, recognizing the influence the spacer region between the Shine-Dalgarno (SD) sequence and the start codon has on Cas9 expression [56, 58, 59], the spacer (5'-CAACAAG-3') of riboswitch E* in pMKR06 was replaced with a shorter spacer (5'-TCCCAT-3') to generate a modified riboswitch E* as well as pMKR07. This spacer is from the high-expression *Streptomyces* plasmids, wzc-orfA and wzc-orfL [48], which were inspired by pNG2 (accession KR131849) [60]. The plasmid pMKR01, which lacks both the *ermE** promoter and *cas9* relative to pMKR08, was also constructed as a control in evaluating the effectiveness of these riboswitches in mitigating Cas9-induced cytotoxicity. SgRNAs targeting both ends of *pikAII* as well as a homologous DNA repair template were introduced into each plasmid, and the recombinant plasmids were introduced into *S. venezuelae* via protoplast-mediated transformation. After a 5-day culture period, high transformation efficiency was observed for pMKR01-pikAII, pMKR02-pikAII, pMKR04-pikAII, pMKR05-pikAII, pMKR06-pikAII, and pMKR07-pikAII, but low transformation efficiency was observed for pMKR03-pikAII and pMKR08-pikAII (Fig. 2). This is presumably due to the relative absence or presence of Cas9. Interestingly, pMKR03-pikAII, which expresses Cas9 under the control of riboswitch B, exhibited the lowest transformation efficiency (about 4%) of the riboswitch-containing systems, suggesting that leaky Cas9 expression caused cell damage, as previously reported [56].

Efficiency of *pikAII* deletions by CRISPR-Cas9 systems

The effectiveness of CRISPR-Cas9-mediated genome editing depends on the generation of Cas9-mediated DSBs and the engagement of an intrinsic HDR system. In our CRISPR-Cas9 systems, Cas9 expression is dependent not only on theophylline concentration but also on the activity of the *ermE** promoter, which is, in turn, dependent on growth conditions(61, 62). Since intracellular ATP levels and HDR efficiency are known to be correlated in *Streptomyces coelicolor*, genome-editing efficiency may be improved in *S. venezuelae* by modulating cellular energy metabolism[40, 63, 64]. Accordingly, we investigated the effects of culture media and theophylline concentrations on the efficiency of our CRISPR-Cas9 systems in *S. venezuelae*. Due to limitations related to solubility and the influence on bacterial growth, the maximum concentration of theophylline used for induction was 4 mM [57, 65, 66]. AS-1, MS, TSB, and SPA agar were examined, as each contains a different type or concentration of carbon sources [53, 67]. The results from the *pikAII*-deletion experiments revealed that CRISPR-Cas9 editing efficiency increased with theophylline concentration and that the highest efficiencies were from induction on SPA medium agar. Remarkably, pMKR07-pikAII (modified riboswitch E*) enabled an 87.5% genetic-editing success rate for the deletion of *pikAII* when transformants were induced on SPA medium agar with 4 mM theophylline (Table 1; Additioanl file 1: Fig. S3). Under the same conditions, pMKR06-pikAII (riboswitch E*) only provided a 25% success rate. Intriguingly, the observed efficacy was not achieved when transformants harboring the pMKR07 system were cultured on AS-1 medium agar, even with identical theophylline induction. These findings underscore the importance of culture media composition and inducer concentration for CRISPR-Cas9-mediated genetic modifications in *S. venezuelae* and suggest higher Cas9 expression under modified riboswitch E* than riboswitch E* post-induction. To further examine the differential effects of riboswitch E* and modified riboswitch

Table 1 Optimizing the deletion of *pikAII* through varying riboswitches, theophylline concentration, and media

	AS-1			MS			TSB			SPA		
Theophylline (mM)	**0**	**2**	**4**	**0**	**2**	**4**	**0**	**2**	**4**	**0**	**2**	
pMKR02-pikAII (riboswitch A)	0/8	0/8	0/8	0/8	0/8	0/8	0/8	0/8	0/8	0/8	0/8	0/8
pMKR03-pikAII (riboswitch B)	0/8	0/8	0/8	0/8	0/8	0/8	0/8	0/8	0/8	0/8	0/8	0/8
pMKR04-pikAII (riboswitch C)	0/8	0/8	0/8	0/8	0/8	0/8	0/8	0/8	0/8	0/8	0/8	0/8
pMKR05-pikAII (riboswitch D)	0/8	0/8	0/8	0/8	0/8	0/8	0/8	0/8	0/8	0/8	0/8	0/8
pMKR06-pikAII (riboswitch E*)	0/8	0/8	0/8	0/8	0/8	1/8	0/8	0/8	1/8	0/8	2/8	2/8
pMKR07-pikAII (modified riboswitch E*)	0/8	0/8	0/8	0/8	1/8	3/8	0/8	0/8	1/8	0/8	3/8	7/8
	Results [a]											

AS-1, MS, TSB, and SPA are the media used for induction. [a]Number of correctly engineered transformants/total number of transformants screened

E* on downstream gene expression following induction, two *gusA*-reporter plasmids, pE*-GusA and pmE*-GusA, were respectively generated from pMKR06 and pMKR07 by replacing *cas9* with *gusA*. Leaky GusA expression was observed from both plasmids after 2 days of culturing without theophylline supplementation. This likely explains the reduced transformation efficiency observed for pMKR06 and pMKR07 compared to pMKR01 (Fig. 2). Furthermore, higher GusA expression was observed for modified riboswitch E* than for riboswitch E* when transformants were cultured on SPA medium agar with 4 mM theophylline for 2 days (Additioanl file 1: Fig. S4). This strongly suggests that the enhanced genetic-editing capability of the pMKR07 system over the pMKR06 system is due to increased Cas9 expression.

Deletion of large DNA regions by the pMKR07 system

To further evaluate the editing capabilities of the pMKR07 system on large DNA regions, a series of deletion experiments targeting *pikAI* (13 kb), *pikAII* (11 kb), the *pikAIII-desVIII* region (11 kb), and the *pikR2-desR* region (47 kb) was conducted. The findings revealed that, while efficiency decreased when deleting larger DNA fragments, the pMKR07 system remained effective deleting DNA segments up to 47 kb in size (20% efficiency) (Table 2) (Additioanl file 1: Fig. S3; S5-S7). Nanopore sequencing indicated that the genomic DNA sequences of gene-deficient mutants were edited precisely as designed without random recombination events (data not shown). Additionally, complementary plasmids, W1, W2, and W3, and the bacterial artificial chromosome (BAC) BP, respectively carrying *pikAI*, *pikAII*, *pikAIII-desVIII*, and *pikR2-resR*, were constructed and introduced into their corresponding genetically-deficient strain. Liquid chromatography/high-resolution mass spectrometry (LC/HRMS) analysis of complemented strain culture extracts confirmed that pikromycin production was restored in each case, substantiating the precise genetic-editing ability of the pMKR07 system (Fig. 3).

Table 2 Genome-editing results employing the pMKR07 system in *S. venezuelae*

Plasmid	Function	Edited region (bp)	Result[a]
pMKR07-pikAI	deleting *pikAI* gene	12,640	7/8
pMKR07-pikAII	deleting *pikAII* gene	10,678	7/8
pMKR07-pikAIII	deleting *pikAIII-desVIII* region	10,596	8/8
pMKR07-pik	deleting *pikR2-desR* region	47,022	3/15
pMKR07-P6E6	swapping module 6 of pikromycin PKS for module 6 of erythromycin PKS	replacing 4,782 bp DNA with 4,377 bp DNA	4/8
pMKR07-P2T2	swapping module 2 of pikromycin PKS for module 2 of tylosin PKS	replacing 4,434 bp DNA with 4,548 bp DNA	3/8
pMKR07-P1V1	swapping module 1 of pikromycin PKS for module 1 of venediol PKS	replacing 4,395 bp DNA with 4,440 bp DNA	2/6

[a] Number of correctly engineered transformants/total number of transformants screened

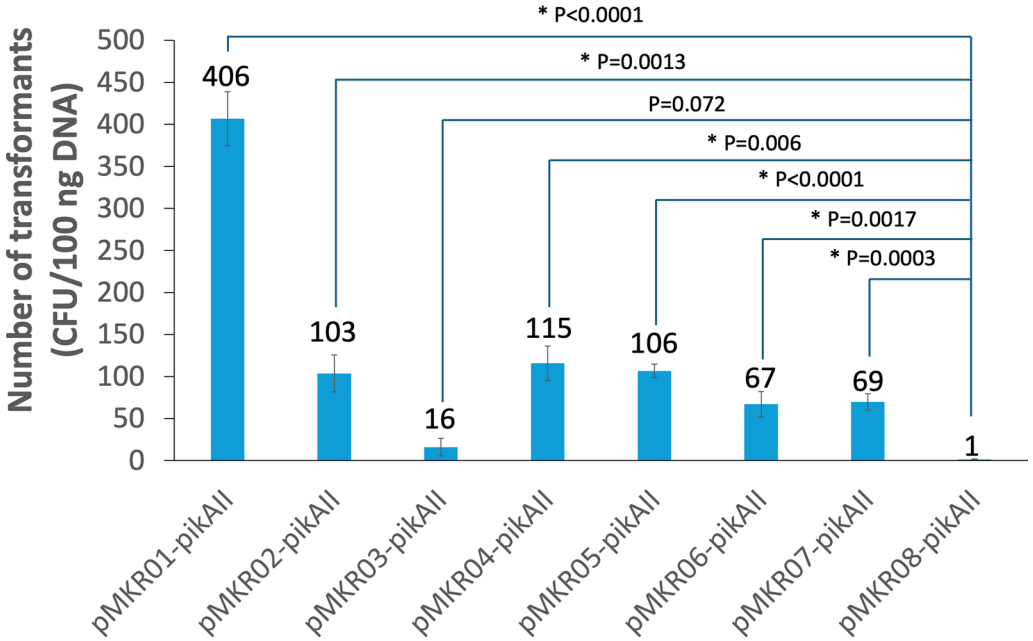

Fig. 2 Transformation efficiencies of CRISPR-Cas9 systems mediating *pikAII* deletion. Each of the plasmids are derived from pMKR08 and contain the same sgRNAs targeting the ends of *pikAII* and homology repair template. pMKR01 does not contain either the *ermE** promoter or *cas9*. pMKR02-pikAII, pMKR03-pikAII, pMKR04-pikAII, pMKR05-pikAII, pMKR06-pikAII, and pMKR07-pikAII respectively contain theophylline-responsive riboswitches **A**–**E*** and a modified **E*** to modulate Cas9 expression. The average number of transformants per 100 ng plasmid (from 3 independent transformations) are reported with standard deviations. Statistical significance was assessed by a two-tailed unpaired Student's t-test, and asterisks show statistically significant differences

A conservative module swap

The pikromycin and erythromycin PKSs are highly similar. The 6th module of each synthase (**P6** and **E6**) performs the same chemistry on highly similar polyketide intermediates. However, they are architecturally distinct in that **E6** is housed on a single polypeptide whereas **P6** is housed by two polypeptides connected through docking domain motifs (Fig. 1A, B). To investigate the interchangeability of these modules the ability of the pMKR07 system to manipulate large genomic regions, we replaced **P6** with **E6** in the *S. venezuelae* genome (see Methods). Following CRISPR-Cas9 editing and plasmid curing, amplicons generated using the P83/P84 primer set and digested with SacI yielded the anticipated fragments (2.6 and 2.4 kb, rather than 3.8 and 1.6 kb for the wild-type strain) (Additioanl file 1: Fig. S8). Sanger sequencing of these amplicons confirmed the module replacement. The **P6**/**E6**-swapped strain, ZC1, was generated with an editing efficiency of 50%. LC/HRMS analysis of ZC1 culture extract indicated production of **1**. This compound was purified and confirmed to be pikromycin by nuclear magnetic resonance (NMR) (Fig. 4A, B, Additioanl file 1: Fig. S9-S12). The ZC1 strain, with its **P6**/**E6**-swapped pikromycin PKS, produces **1** with a yield of 20 mg/L (80% the wild-type level).

Module swaps yield two bioactive pikromycin derivatives

In the biosyntheses of pikromycin and the related macrolide antibiotic tylosin, the 2nd modules of their respective PKSs (**P2** and **T2**) generate α-methyl, β-hydroxy diketide intermediates; however, their α-methyl groups are oppositely oriented [68] (Fig. 1C). We aimed to reverse the stereochemistry of corresponding methyl group at the C12 position of pikromycin through a **P2**/**T2**-swap and generated the strain ZC2 (Additioanl file 1: Fig. S13). Following a 2-day fermentation, low levels (0.15 mg/L) of a compound with a molecular weight corresponding to narbomycin, were detected (Fig. 4C, D). Compound **3** was isolated and characterized by NMR spectroscopy (Figs. S14-S17) and chiral LC/HRMS (Fig. 5).

Structural modification at the C13 position of macrolide antibiotics has yielded derivatives with enhanced activity against resistant bacterial pathogens [69, 70]. In contrast to the 1st module of the pikromycin synthase (**P1**) that generates a propionyl starter unit, the 1st module of the venediol PKS (**V1**), also encoded on the *S. venezuelae* ATCC 15439 genome, generates an acetyl starter unit. A swap of these modules could yield a methyl rather than an ethyl substituent at the C13 position of pikromycin. The **P1**/**V1**-swapped strain, ZC3, was engineered, and PCR analyses indicated a

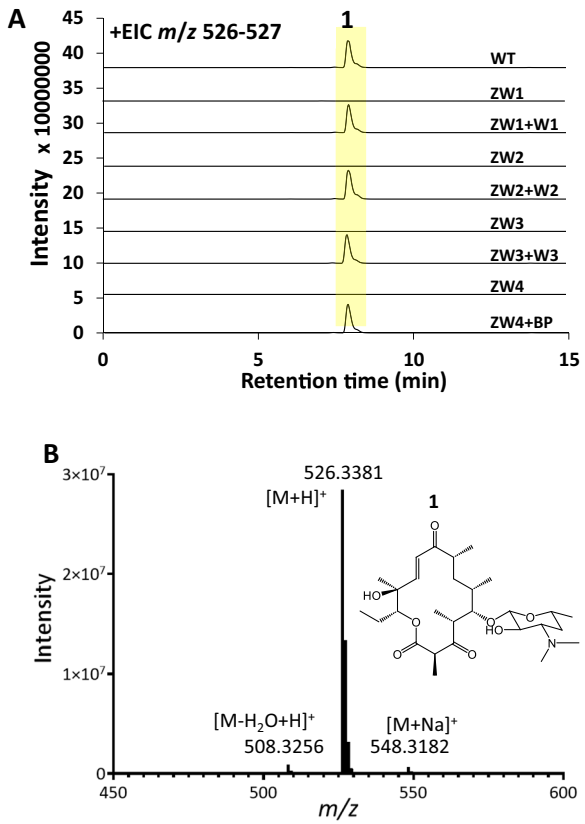

Fig. 3 LC/HRMS analysis shows complementation of gene-deleted strains restores pikromycin production. **A** Extracted ion chromatograms (EICs) of pikromycin (**1**) from the culture extracts of *S. venezuelae* ATCC 15439, gene-deleted strains, and complemented strains. WT: *S. venezuelae* ATCC 15439; ZW1: *pikAI*-deleted strain; ZW2: *pikAII*-deleted strain; ZW3: *pikAIII-desVIII*-deleted strain; ZW4: *pikR2-resR*-deleted strain. W1, W2, W3, and BP: Plasmids/BAC carrying *pikAI*, *pikAII*, *pikAIII-desVIII*, and *pikR2-resR* for restoring pikromycin production through complementation. **B** Electrospray ionization (ESI) mass spectrum of **1** from the *S. venezuelae* ATCC 15439 culture extract. **1**, $[M+H]^+$ observed: 526.3381 *m/z*, expected: 526.3380 *m/z*, 0.19 ppm)

Cas9-editing efficiency of 33% (Fig. 1D; Additioanl file 1: Fig. S18, Table 2) [42]. A substantial fraction of the mutants remained resistant to apramycin after curing the CRISPR-Cas9 plasmid (pMKR07-P1V1). We hypothesize this is due to the integration of the plasmid into the *S. venezuelae* genome, facilitated by the homologous DNA fragment of the **V1** module carried on the plasmid. After 2 days of culturing, ZC3 produced compound **4** (7.5 mg/L, 30% of **1** from *S. venezuelae* ATCC 15439), whose HRMS and NMR spectra are consistent with the anticipated C13-methyl derivative of pikromycin (Fig. 4E, F, Additioanl file 1: Fig. S19-S22).

The antimicrobial activities of **3** and **4** against *Bacillus subtilis* were compared to those of pikromycin (**1**) and narbomycin (**2**, provided by Takeshi Miyazawa) [71] (Additioanl file 1: Fig. S23, Table 3). MIC measurements show they are half as active.

Discussion

Synthetic biologists primarily choose between two approaches when engineering hybrid natural product pathways. The first is to place genes from biosynthetic pathways on vectors, such as plasmids, BACs, or yeast artificial chromosomes, and express them in heterologous hosts; however, problems often arise due to host incompatibilities, limited precursors, complex regulation, and toxicity [14, 32, 39, 72, 73]. The second approach is to directly edit the genomes of native producer strains [37, 74–76]. This can maintain the native regulatory mechanisms and metabolic infrastructure of the host but is more technically challenging. To accelerate the genome modification of streptomycetes, researchers have developed various strategies, including using alternative endonucleases (*e.g.*, Cas3, Cas12a) and decoupling the transformation and editing steps through inducible Cas9 expression [77–80]. Despite these advances, modifying large DNA regions within genomes has remained a challenge [38].

In this work, 6 theophylline-responsive riboswitches (A-E* and modified E*) were employed to minimize cytotoxicity from Cas9 during transformation and maximize the frequency of genome modification after Cas9 induction (Additioanl file 1: Fig. S1) [56]. Riboswitch B resulted in the lowest transformation efficiency, suggesting that Cas9 expression was leaky and cytotoxic. No *pikAII*-deletion mutants were observed when employing pMKR03-pikAII under various culture conditions, either in the presence and absence of theophylline. As previous studies with riboswitch B in *S. coelicolor* observed leaky expression, leaky Cas9 expression may have impeded cell growth [81]. Although plasmids harboring riboswitches A, C, and D show high transformation efficiencies, they also did not yield *pikAII*-deletion mutants, even after culturing with various media supplemented with theophylline. From research on theophylline-responsive riboswitches in *S. coelicolor* [57], we hypothesize post-induction Cas9 expression levels were insufficient. From the results of the GusA reporter assay (Additioanl file 1: Fig. S3), we hypothesize that higher genetic-editing capability correlates with post-induction Cas9 expression levels. Furthermore, our tests on the effects of various culture media on genetic editing revealed higher editing efficiency when transformants were cultured and induced on nutrient-rich medium agar plates that promoted faster growth. Bacterial aerobic respiration generates ATP through the metabolic processes of glycolysis and oxidative phosphorylation. The available carbon

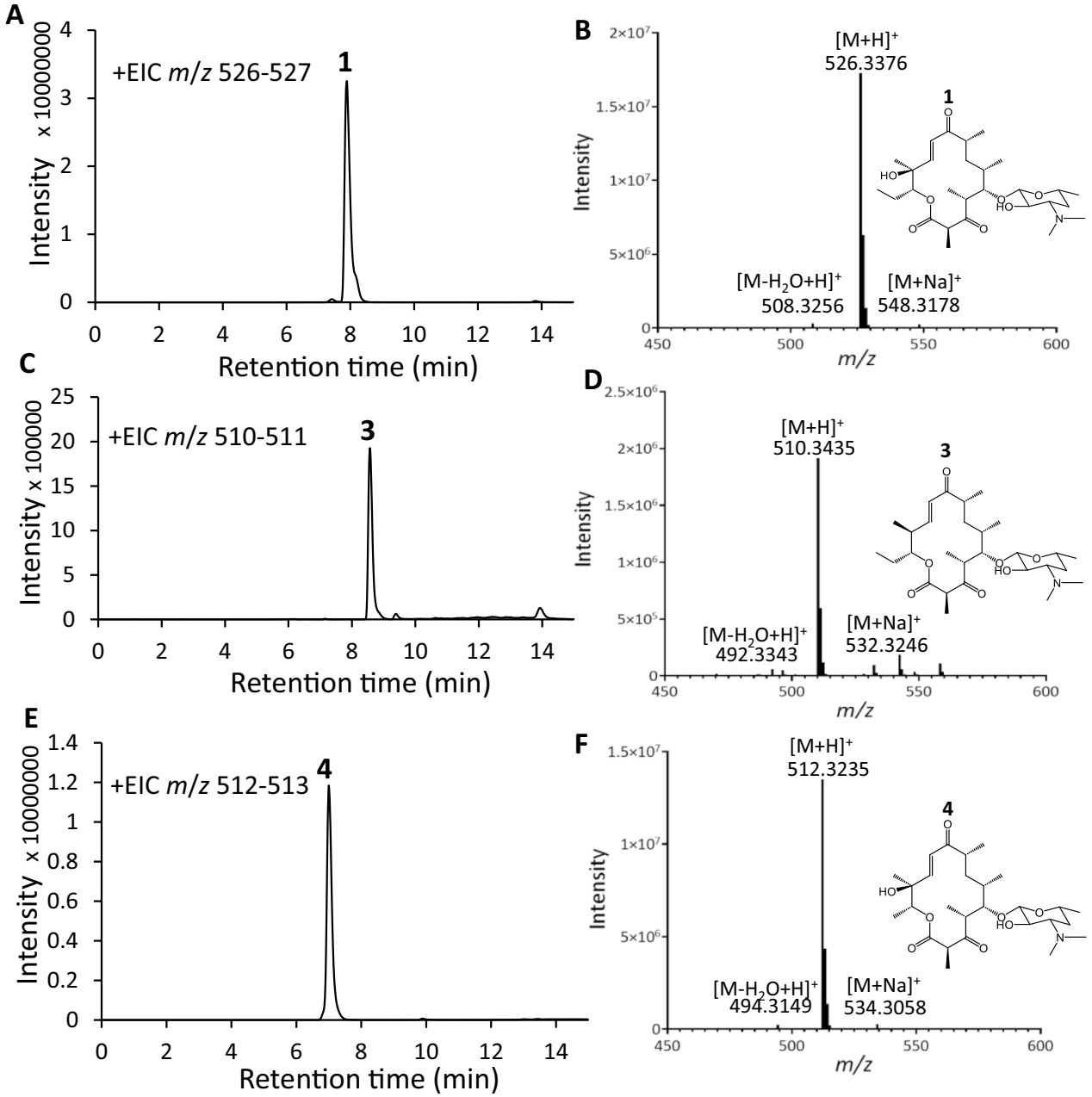

Fig. 4 LC/HRMS analysis of **1**, **3**, and **4** production by strains harboring module-swapped pikromycin PKSs. **A** EIC (*m/z* 526–527, anticipated for **1**) from the culture extract of **P6**/**E6**-swapped ZC1. **B** Mass spectrum of **1** from ZC1. **C** EIC (*m/z* 510–511, anticipated for **3**) from the culture extract of **P2**/**T2**-swapped ZC2. **D** Mass spectrum of **3** from ZC2. **E** EIC (*m/z* 512–513, anticipated for **4**) from the culture extract of **P1**/**V1**-swapped ZC3. **F** Mass spectrum of **4** from ZC3. **1**, $[M+H]^+$ observed: 526.3376 *m/z*, expected: 526.3380 *m/z*, –0.76 ppm); **3**, $[M+H]^+$ observed: 510.3435 *m/z*, expected: 510.3431 *m/z*, 0.78 ppm); **4**, $[M+H]^+$ observed: 512.3235 *m/z*, expected: 512.3223 *m/z*, 2.34 ppm)

sources, especially glucose as the primary energy substrate for cellular metabolism, significantly influence ATP levels [64, 82, 83]. The pMKR07 system demonstrated the highest efficiency deleting *pikAII* when transformants were cultured and induced on SPA medium agar, which has a higher glucose concentration than TSB or MS medium agar. These results show that genome editing is influenced by Cas9 levels and nutrient metabolism. The pMKR07 system reliably performed 4–5 kb swaps, enabling the **P6**/**E6**, **P2**/**T2**, and **P1**/**V1** replacements with success rates of 50%, 37.5%, and 33%, respectively (Table 2). Although these rates are lower than those

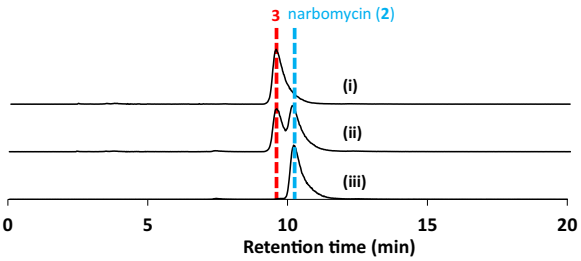

Fig. 5 Chromatographic separation between narbomycin and narbomycin epimer **3**. EICs are shown from chiral LC/HRMS analysis of (i) **3**, (ii) a mixture of **3** and narbomycin (**2**), and (iii) **2**

Table 3 MIC[a] values for macrolides **1**–**4**

Bacteria	pikromycin (1)	narbomycin (2)	3	4
B. subtilis strain 168	12.5 μM	12.5 μM	25 μM	25 μM

[a] MIC is defined as the lowest concentration of analyte with no visible growth

observed when knocking out *pikAI* (13 kb, 87.5%), *pikAII* (11 kb, 87.5%), and *pikAIII-desVIII* (11 kb, 100%), they surpass the efficiency of deleting the entire pikromycin biosynthetic gene cluster (47 kb, 20%). HDR-mediated modifications of large DNA regions are known to occur at lower rates than HDR-mediated small deletions, insertions, and substitutions [84].

The yield of pikromycin (**1**) from the **P6**/**E6**-swapped ZC1 is 80% that of wild-type. As studies indicate *pikAIV* is co-transcribed with *pikAIII* (Fig. 3B), the **P6**/**E6** swap may not affect the level of mRNA encoding this region of the synthase [85]. However, it does result in the production of a 308 kDa hybrid polypeptide rather than PikAIII (164 kDa) and PikAIV (142 kDa) (Fig. 1B). Since transcript length is a key determinant of translation efficiency, the hybrid polypeptide may be present at decreased levels [86, 87]. The relative decrease in pikromycin titer could also be related to suboptimal interactions between **E6** and the rest of the pikromycin PKS or the intermediates on which it operates, although a recent study observed similar activities from **P6** and **E6** within engineered PKSs [11, 88].

Module-swapping with the pMKR07 system enabled strains ZC2 and ZC3 to generate new macrolide antibiotics. **P2**/**T2**-swapped ZC2 produces low levels of **3**, the C12-epimer of narbomycin. LC/HRMS analysis of the ZC2 culture extract does not show any compound with the same *m*/*z* as pikromycin (**1**). Thus, likely due to the orientation of its C12 methyl group, **3** is not a substrate for PikC, which naturally oxidizes the C12 position of narbomycin [89]. The low titer of **3** could be a result of its oppositely-oriented C12 methyl group causing suboptimal interactions between intermediates and downstream PKS enzymes, such as the triketide intermediate with the **P3** KS or the heptaketide intermediate with the thioesterase (TE) [16, 90]. **P1**/**V1**-swapped ZC3 produces pikromycin derivative **4**, which contains a methyl rather than an ethyl group at C13, at a level similar to that of **1** from *S. venezuelae* ATCC 15439. Apparently, the intermediates of the **P1**/**V1**-swapped pikromycin PKS, which are one methylene group shorter than those of the native synthase, are well tolerated by the hybrid PKS. Also, the narbonolide derivatives generated by the **P2**/**T2** and **P1**/**V1**-swapped PKSs are desosaminylated by DesVII/DesVIII, known to be relatively promiscuous, as these derivatives were not observed from the LC/HRMS analyses of the culture extracts [91].

The new macrolide antibiotics **3** and **4** show bioactivities comparable to the natural ketolides pikromycin (**1**) and narbomycin (**2**). As these compounds possess alterations to the region that is converted to a carbamate, carbonate, or lactone in semisynthetic ketolides (e.g., telithromycin), they may be of interest to medicinal chemists [92, 93]. Modifications at the C13 position of macrolide antibiotics, such as clarithromycin, can improve their bioactivities through enhanced hydrophobic interactions with the ribosome [70]. It may be possible to increase the size and lipophilicity of the C13 substituent by replacing **P1** with the first modules of other synthases, such as the borrelidin or rapamycin PKS [94, 95].

CRISPR-Cas9 technology offers considerable advantages but also presents notable limitations, particularly the risk of off-target effects. These events occur when Cas9 unintentionally induces DSBs at genomic loci with sequence similarity to the intended target [96]. Whole genome sequencing of the edited mutants revealed several mismatched nucleotides across the entire genome, including areas outside the pikromycin biosynthetic gene cluster. These mismatches may result from spontaneous mutations or sequencing artifacts; however, no large-scale insertions, deletions, or genomic rearrangements were detected. To reduce off-target activity, high-fidelity Cas9 variants, such as eSpCas9 and SpCas9-HF1 have been developed, albeit often at the cost of decreased on-target efficiency [97, 98]. Despite these advances, eliminating off-target effects remains a significant challenge. This emphasizes the need for comprehensive off-target assessments and the implementation of risk mitigation strategies in CRISPR-based applications.

Over the past few decades, various inducible promoter systems have been used to temporally regulate the expression of target genes in *Streptomyces* [99–107]. These inducible systems are essential to mitigate the cytotoxic effects associated with target gene expression

until the cells reach a specific physiological state, such as a particular growth phase or culture density. Conventional induction strategies utilize antibiotics (e.g., thiostrepton, tetracycline, oxytetracycline) [99–101], sugars (e.g., xylose, rhamnose, cellobiose) [102–104], and small molecules (e.g., cumate, resorcinol, ε-caprolactam) [105–107]. However, these approaches suffer from intrinsic limitations: antibiotic inducers can provoke cellular stress responses and off-target gene activation [108]; sugar inducers may be metabolized or synthesized endogenously [103, 109, 110], complicating dose control; and certain chemical effectors pose biosafety concerns [111]. Moreover, many inducible promoters exhibit low transcriptional output and frequently require co-expression of resistance markers or accessory regulatory proteins [99, 100, 105, 112]. Herein, we introduced a theophylline-responsive riboswitch that obviates the need for accessory protein factors by relying exclusively on a non-metabolizable ligand for precise, dose-dependent modulation of Cas9 expression. Our system maintains negligible basal Cas9 activity in the absence of theophylline and eliminates the requirement for additional repressors or antibiotic resistance genes. We demonstrated that this riboswitch-based platform markedly improves transformation efficiency while retaining stringent specificity [81]. This implementation therefore provides a robust, clean, and highly tunable alternative for inducible genome engineering.

Conclusions

Developing the pMKR07 CRISPR-Cas9 system with a segregationally-unstable origin of replication and modified theophylline-responsive riboswitch as well as employing it in optimized growth conditions enabled the efficient and precise editing of large DNA regions within *S. venezuelae* ATCC 15439. These findings open opportunities for developing similar systems for editing the genomes of other streptomycetes. The ability to perform module-swapping of the pikromycin PKS and related assembly lines within their native hosts will not only enable scientists to learn more about assembly line logic and engineering but also facilitate the generation of new medicines.

Abbreviations

PKS	Polyketide synthase
AT	Acyltransferase
ACP	Acyl carrier protein
KS	Ketosynthase
KR	Ketoreductase
DH	Dehydratase
ER	Enoylreductase
TE	Thioesterase
KS^Q	KS-like decarboxylase
KR^0	KR-like epimerase
CRISPR	Clustered regularly interspaced short palindromic repeats
Cas9	CRISPR-associated protein 9
sgRNA	Single-guide RNA
PAM	Protospacer adjacent motif
BAC	Bacterial artificial chromosome
EIC	Extracted ion chromatogram
DSB	Double-strand DNA break
NHEJ	Non-homologous end-joining
P1-P7	The 7 modules of the pikromycin PKS
E6	The 6th module of the erythromycin PKS
T2	The 2nd module of the tylosin PKS
V1	The 1st module of the venediol PKS
DesVII/DesVIII	The desosaminyltransferase in the pikromycin pathway
PikC	The cytochrome P450 hydroxylase in the pikromycin pathway
X-gluc	5-Bromo-4-chloro-3-indolyl-beta-D-glucuronic acid
SD	Shine-Dalgarno
NMR	Nuclear magnetic resonance
PCR	Polymerase chain reaction
ATP	Adenosine 5′-triphosphate
LC/HRMS	Liquid chromatography/high-resolution mass spectrometry

Supplementary Information

The online version contains supplementary material available at https://doi.org/10.1186/s12934-025-02741-w.

Supplementary Material 1.

Acknowledgements

We thank Po-Hsun Fan of the Department of Chemistry at The University of Texas at Austin for help with HPLC purification and analysis. Cartoon illustrations were created using the BioRender.com website.

Author contributions

ATK initiated the project and designed experiments. ZCW performed gene cloning, reporter assay and MIC assay. ZCW and HS performed chemical isolation, LC/HRMS, structural confirmations, and drafted the manuscript. ATK revised the manuscript. TM initiated the swapping experiments and provided compounds.

Funding

This work was supported by the NIH (GM145992).

Availability of data and materials

No datasets were generated or analysed during the current study. The pMKR07 plasmid is available through addgene (#240097).

Declarations

Ethics approval and consent to participate

Not applicable.

Consent for publication

Not applicable.

Competing interests

The authors declare no competing interests.

Received: 14 March 2025 Accepted: 6 May 2025
Published online: 27 May 2025

References

1. Alam K, Mazumder A, Sikdar S, Zhao YM, Hao J, Song C, et al. Streptomyces: the biofactory of secondary metabolites. Front Microbiol. 2022;13:968053.
2. Hobson D. Activity of erythromycin against *Staphylococcus aureus*. Br Med J. 1954;1(4856):236–9.
3. Ganesh SK, Subathra DC. Molecular and therapeutic insights of rapamycin: a multi-faceted drug from Streptomyces hygroscopicus. Mol Biol Rep. 2023;50(4):3815–33.
4. Risdian C, Mozef T, Wink J. Biosynthesis of polyketides in streptomyces. Microorganisms. 2019;7(5):124.
5. Nivina A, Yuet KP, Hsu J, Khosla C. Evolution and diversity of assembly-line polyketide synthases. Chem Rev. 2019;119(24):12524–47.
6. Dutta S, Whicher JR, Hansen DA, Hale WA, Chemler JA, Congdon GR, et al. Structure of a modular polyketide synthase. Nature. 2014;510(7506):512–7.
7. Keatinge-Clay AT. The structures of type I polyketide synthases. Nat Prod Rep. 2012;29(10):1050–73.
8. Klaus M, Grininger M. Engineering strategies for rational polyketide synthase design. Nat Prod Rep. 2018;35(10):1070–81.
9. Menzella HG, Reid R, Carney JR, Chandran SS, Reisinger SJ, Patel KG, et al. Combinatorial polyketide biosynthesis by de novo design and rearrangement of modular polyketide synthase genes. Nat Biotechnol. 2005;23(9):1171–6.
10. Zhang L, Hashimoto T, Qin B, Hashimoto J, Kozone I, Kawahara T, et al. Characterization of giant modular PKSs provides insight into genetic mechanism for structural diversification of aminopolyol polyketides. Angew Chem Int Ed Engl. 2017;56(7):1740–5.
11. Ray KA, Saif N, Keatinge-Clay AT. Modular polyketide synthase ketosynthases collaborate with upstream dehydratases to install double bonds. Chem Commun (Camb). 2024;60(66):8712–5.
12. Buyachuihan L, Zhao Y, Schelhas C, Grininger M. Docking domain engineering in a modular polyketide synthase and its impact on structure and function. ACS Chem Biol. 2023;18(7):1500–9.
13. Peng H, Ishida K, Sugimoto Y, Jenke-Kodama H, Hertweck C. Emulating evolutionary processes to morph aureothin-type modular polyketide synthases and associated oxygenases. Nat Commun. 2019;10(1):3918.
14. Miyazawa T, Hirsch M, Zhang Z, Keatinge-Clay AT. An in vitro platform for engineering and harnessing modular polyketide synthases. Nat Commun. 2020;11(1):80.
15. Miyazawa T, Fitzgerald BJ, Keatinge-Clay AT. Preparative production of an enantiomeric pair by engineered polyketide synthases. Chem Commun (Camb). 2021;57(70):8762–5.
16. Ray KA, Lutgens JD, Bista R, Zhang J, Desai RR, Hirsch M, et al. Assessing and harnessing updated polyketide synthase modules through combinatorial engineering. Nat Commun. 2024;15(1):6485.
17. Hoff G, Bertrand C, Piotrowski E, Thibessard A, Leblond P. Genome plasticity is governed by double strand break DNA repair in Streptomyces. Sci Rep. 2018;8(1):5272.
18. Ye SH, Enghiad B, Zhao HM, Takano E. Fine-tuning the regulation of Cas9 expression levels for efficient CRISPR-Cas9 mediated recombination in. J Ind Microbiol Biot. 2020;47(4–5):413–23.
19. Komor AC, Kim YB, Packer MS, Zuris JA, Liu DR. Programmable editing of a target base in genomic DNA without double-stranded DNA cleavage. Nature. 2016;533(7603):420.
20. Tong Y, Jorgensen TS, Whitford CM, Weber T, Lee SY. A versatile genetic engineering toolkit for *E. coli* based on CRISPR-prime editing. Nat Commun. 2021;12(1):5206.
21. Anzalone AV, Gao XD, Podracky CJ, Nelson AT, Koblan LW, Raguram A, et al. Programmable deletion, replacement, integration and inversion of large DNA sequences with twin prime editing. Nat Biotechnol. 2022;40(5):731–40.
22. Anzalone AV, Randolph PB, Davis JR, Sousa AA, Koblan LW, Levy JM, et al. Search-and-replace genome editing without double-strand breaks or donor DNA. Nature. 2019;576(7785):149–57.
23. Nahvi A, Sudarsan N, Ebert MS, Zou X, Brown KL, Breaker RR. Genetic control by a metabolite binding mRNA. Chem Biol. 2002;9(9):1043.
24. Sudarsan N, Barrick JE, Breaker RR. Metabolite-binding RNA domains are present in the genes of eukaryotes. RNA. 2003;9(6):644–7.
25. Mandal M, Breaker RR. Gene regulation by riboswitches. Nat Rev Mol Cell Biol. 2004;5(6):451–63.
26. Kavita K, Breaker RR. Discovering riboswitches: the past and the future. Trends Biochem Sci. 2023;48(2):119–41.
27. Breaker RR. The Biochemical Landscape of Riboswitch Ligands. Biochemistry. 2022;61(3):137–49.
28. Suess B, Fink B, Berens C, Stentz R, Hillen W. A theophylline responsive riboswitch based on helix slipping controls gene expression in vivo. Nucleic Acids Res. 2004;32(4):1610–4.
29. Wrist A, Sun W, Summers RM. The theophylline aptamer: 25 years as an important tool in cellular engineering research. ACS Synth Biol. 2020;9(4):682–97.
30. Vandierendonck J, Girardin Y, De Bruyn P, De Greve H, Loris R. A multilayer-controlled strategy for cloning and expression of toxin genes in *Escherichia coli*. Toxins (Basel). 2023;15(8):508.
31. Fernandes P, Martens E, Pereira D. Nature nurtures the design of new semi-synthetic macrolide antibiotics. J Antibiot (Tokyo). 2017;70(5):527–33.
32. Yoon YJ, Beck BJ, Kim BS, Kang HY, Reynolds KA, Sherman DH. Generation of multiple bioactive macrolides by hybrid modular polyketide synthases in Streptomyces venezuelae. Chem Biol. 2002;9(2):203–14.
33. Kim BS, Sherman DH, Reynolds KA. An efficient method for creation and functional analysis of libraries of hybrid type I polyketide synthases. Protein Eng Des Sel. 2004;17(3):277–84.
34. Xue Y, Sherman DH. Biosynthesis and combinatorial biosynthesis of pikromycin-related macrolides in *Streptomyces venezuelae*. Metab Eng. 2001;3(1):15–26.
35. Gupta S, Lakshmanan V, Kim BS, Fecik R, Reynolds KA. Generation of novel pikromycin antibiotic products through mutasynthesis. ChemBioChem. 2008;9(10):1609–16.
36. Pang B, Graziani EI, Keasling JD. Acyltransferase domain swap in modular type I polyketide synthase to adjust the molecular gluing strength of rapamycin. Tetrahedron Lett. 2022;112:154229.
37. Thong WL, Zhang Y, Zhuo Y, Robins KJ, Fyans JK, Herbert AJ, et al. Gene editing enables rapid engineering of complex antibiotic assembly lines. Nat Commun. 2021;12(1):6872.
38. Lee Y, Hwang S, Kim W, Kim JH, Palsson BO, Cho BK. CRISPR-aided genome engineering for secondary metabolite biosynthesis in Streptomyces. J Ind Microbiol Biotechnol. 2024. https://doi.org/10.1093/jimb/kuae009.
39. Kudo K, Hashimoto T, Hashimoto J, Kozone I, Kagaya N, Ueoka R, et al. In vitro Cas9-assisted editing of modular polyketide synthase genes to produce desired natural product derivatives. Nat Commun. 2020;11(1):4022.
40. Wang K, Zhao QW, Liu YF, Sun CF, Chen XA, Burchmore R, et al. Multi-layer controls of Cas9 activity coupled with ATP synthase over-expression for efficient genome editing in streptomyces. Front Bioeng Biotechnol. 2019;7:304.
41. Li S, Li Z, Zhang G, Urlacher VB, Ma L, Li S. Functional analysis of the whole CYPome and Fdxome of *Streptomyces venezuelae* ATCC 15439. Eng Microbiol. 2024;4(4):100166.
42. Li S, Chi LP, Li Z, Liu MY, Liu RX, Sang ML, et al. Discovery of venediols by activation of a silent type I polyketide biosynthetic gene cluster in ATCC 15439. Tetrahedron. 2022;126.
43. Mo J, Wang S, Zhang W, Li C, Deng Z, Zhang L, et al. Efficient editing DNA regions with high sequence identity in actinomycetal genomes by a CRISPR-Cas9 system. Synth Syst Biotechnol. 2019;4(2):86–91.
44. Kieser T, Bibb MJ, Chater KF, Butter MJ, Hopwood DA, Bittner M, et al. Practical Streptomyces genetics. John Innes Foundation, Norwich, England. 2000.
45. Maezawa I, Kinumaki A, Suzuki M. Letter: Isolation and identification of picronolide, methynolide and neomethynolide produced by *Streptomyces venezuelae* MCRL-0376. J Antibiot (Tokyo). 1974;27(1):84–5.
46. Baltz RH. Genetic recombination in *Streptomyces fradiae* by protoplast fusion and cell regeneration. J Gen Microbiol. 1978;107(1):93–102.
47. Cobb RE, Wang YJ, Zhao HM. High-efficiency multiplex genome editing of species using an engineered CRISPR/Cas system. Acs Synth Biol. 2015;4(6):723–8.
48. Wang ZC, Lo IW, Lin KH, Cheng AN, Zadeh SM, Huang YH, et al. Genetic and Biochemical Characterization of Halogenation and Drug Transportation Genes Encoded in the Albofungin Biosynthetic Gene Cluster. Appl Environ Microbiol. 2022;88(17): e0080622.

49. Sun YH, He XY, Liang JD, Zhou XF, Deng ZX. Analysis of functions in plasmid pHZ1358 influencing its genetic and structural stability in 1326. Appl Microbiol Biot. 2009;82(2):303–10.
50. Cong L, Ran FA, Cox D, Lin S, Barretto R, Habib N, et al. Multiplex genome engineering using CRISPR/Cas systems. Science. 2013;339(6121):819–23.
51. Jinek M, Chylinski K, Fonfara I, Hauer M, Doudna JA, Charpentier E. A programmable dual-RNA-guided DNA endonuclease in adaptive bacterial immunity. Science. 2012;337(6096):816–21.
52. Psenicnik A, Rebersek R, Slemc L, Godec T, Kranjc L, Petkovic H. Simple and reliable in situ CRISPR-Cas9 nuclease visualization tool is ensuring efficient editing in Streptomyces species. J Microbiol Methods. 2022;200: 106545.
53. Pyeon HR, Nah HJ, Kang SH, Choi SS, Kim ES. Heterologous expression of pikromycin biosynthetic gene cluster using Streptomyces artificial chromosome system. Microb Cell Fact. 2017;16(1):96.
54. Wlodek A, Kendrew SG, Coates NJ, Hold A, Pogwizd J, Rudder S, et al. Diversity oriented biosynthesis via accelerated evolution of modular gene clusters. Nat Commun. 2017;8(1):1206.
55. Zhao Y, Li G, Chen Y, Lu Y. Challenges and advances in genome editing technologies in streptomyces. Biomolecules. 2020;10(5):734.
56. Topp S, Reynoso CMK, Seeliger JC, Goldlust IS, Desai SK, Murat D, et al. Synthetic riboswitches that induce gene expression in diverse bacterial species. Appl Environ Microb. 2011. https://doi.org/10.1128/AEM.00247-11.
57. Rudolph MM, Vockenhuber MP, Suess B. Conditional control of gene expression by synthetic riboswitches in Streptomyces coelicolor. Methods Enzymol. 2015;550:283–99.
58. Berwal SK, Sreejith RK, Pal JK. Distance between RBS and AUG plays an important role in overexpression of recombinant proteins. Anal Biochem. 2010;405(2):275–7.
59. Komarova ES, Chervontseva ZS, Osterman IA, Evfratov SA, Rubtsova MP, Zatsepin TS, et al. Influence of the spacer region between the Shine-Dalgarno box and the start codon for fine-tuning of the translation efficiency in *Escherichia coli*. Microb Biotechnol. 2020;13(4):1254–61.
60. Gonzalez-Quinonez N, Lopez-Garcia MT, Yague P, Rioseras B, Pisciotta A, Alduina R, et al. New PhiBT1 site-specific integrative vectors with neutral phenotype in Streptomyces. Appl Microbiol Biotechnol. 2016;100(6):2797–808.
61. Li S, Wang J, Li X, Yin S, Wang W, Yang K. Genome-wide identification and evaluation of constitutive promoters in streptomycetes. Microb Cell Fact. 2015;14:172.
62. Keren L, Zackay O, Lotan-Pompan M, Barenholz U, Dekel E, Sasson V, et al. Promoters maintain their relative activity levels under different growth conditions. Mol Syst Biol. 2013;9:701.
63. Mempin R, Tran H, Chen C, Gong H, Kim Ho K, Lu S. Release of extracellular ATP by bacteria during growth. BMC Microbiol. 2013;13:301.
64. Deng Y, Beahm DR, Ionov S, Sarpeshkar R. Measuring and modeling energy and power consumption in living microbial cells with a synthetic ATP reporter. BMC Biol. 2021;19(1):101.
65. Desai SK, Gallivan JP. Genetic screens and selections for small molecules based on a synthetic riboswitch that activates protein translation. J Am Chem Soc. 2004;126(41):13247–54.
66. Cysewski P, Jelinski T, Cymerman P, Przybylek M. Solvent screening for solubility enhancement of theophylline in neat, binary and ternary NADES solvents: new measurements and ensemble machine learning. Int J Mol Sci. 2021;22(14):7347.
67. Kancharla P, Lu W, Salem SM, Kelly JX, Reynolds KA. Stereospecific synthesis of 23-hydroxyundecylprodiginines and analogues and conversion to antimalarial premarineosins via a Rieske oxygenase catalyzed bicyclization. J Org Chem. 2014;79(23):11674–89.
68. Keatinge-Clay AT. A tylosin ketoreductase reveals how chirality is determined in polyketides. Chem Biol. 2007;14(8):898–908.
69. Ashley GW, Burlingame M, Desai R, Fu H, Leaf T, Licari PJ, et al. Preparation of erythromycin analogs having functional groups at C-15. J Antibiot (Tokyo). 2006;59(7):392–401.
70. Qin Y, Song D, Teng Y, Liu X, Zhang P, Zhang N, et al. Design, synthesis and structure-activity relationships of novel N11-, C12- and C13-substituted 15-membered homo-aza-clarithromycin derivatives against various resistant bacteria. Bioorg Chem. 2021;113: 104992.
71. Keatinge-Clay A, Miyazawa T. Refactoring the pikromycin synthase for the modular biosynthesis of macrolide antibiotics in *E. coli*. Res Sq. 2025. https://doi.org/10.21203/rs.3.rs-5640596/v1.
72. Jiang M, Pfeifer BA. Metabolic and pathway engineering to influence native and altered erythromycin production through *E. coli*. Metab Eng. 2013;19:42–9.
73. Park HS, Park JH, Kim HJ, Kang SH, Choi SS, Kim ES. BAC cloning and heterologous expression of a giant biosynthetic gene cluster encoding antifungal neotetrafibricin in *Streptomyces rubrisoli*. Front Bioeng Biotechnol. 2022;10: 964765.
74. Kim MS, Cho WJ, Song MC, Park SW, Kim K, Kim E, et al. Engineered biosynthesis of milbemycins in the avermectin high-producing strain *Streptomyces avermitilis*. Microb Cell Fact. 2017;16(1):9.
75. Zhang J, Yan YJ, An J, Huang SX, Wang XJ, Xiang WS. Designed biosynthesis of 25-methyl and 25-ethyl ivermectin with enhanced insecticidal activity by domain swap of avermectin polyketide synthase. Microb Cell Fact. 2015;14:152.
76. Li M, Chen Z, Lin X, Zhang X, Song Y, Wen Y, et al. Engineering of avermectin biosynthetic genes to improve production of ivermectin in *Streptomyces avermitilis*. Bioorg Med Chem Lett. 2008;18(20):5359–63.
77. Zimmermann A, Prieto-Vivas JE, Cautereels C, Gorkovskiy A, Steensels J, Van de Peer Y, et al. A Cas3-base editing tool for targetable in vivo mutagenesis. Nat Commun. 2023;14(1):3389.
78. Meliawati M, Schilling C, Schmid J. Recent advances of Cas12a applications in bacteria. Appl Microbiol Biotechnol. 2021;105(8):2981–90.
79. Vento JM, Crook N, Beisel CL. Barriers to genome editing with CRISPR in bacteria. J Ind Microbiol Biotechnol. 2019;46(9–10):1327–41.
80. Alberti F, Corre C. Editing streptomycete genomes in the CRISPR/Cas9 age. Nat Prod Rep. 2019;36(9):1237–48.
81. Rudolph MM, Vockenhuber MP, Suess B. Synthetic riboswitches for the conditional control of gene expression in *Streptomyces coelicolor*. Microbiology (Reading). 2013;159(Pt 7):1416–22.
82. Mu X, Evans TD, Zhang F. ATP biosensor reveals microbial energetic dynamics and facilitates bioproduction. Nat Commun. 2024;15(1):5299.
83. Bonora M, Patergnani S, Rimessi A, De Marchi E, Suski JM, Bononi A, et al. ATP synthesis and storage. Purinergic Signal. 2012;8(3):343–57.
84. Cox DB, Platt RJ, Zhang F. Therapeutic genome editing: prospects and challenges. Nat Med. 2015;21(2):121–31.
85. Wilson DJ, Xue Y, Reynolds KA, Sherman DH. Characterization and analysis of the PikD regulatory factor in the pikromycin biosynthetic pathway of *Streptomyces venezuelae*. J Bacteriol. 2001;183(11):3468–75.
86. Fernandes LD, Moura APS, Ciandrini L. Gene length as a regulator for ribosome recruitment and protein synthesis: theoretical insights. Sci Rep. 2017;7(1):17409.
87. Kumar A, Balbach J. Real-time protein NMR spectroscopy and investigation of assisted protein folding. Biochim Biophys Acta. 2015;1850(10):1965–72.
88. Hirsch M, Fitzgerald BJ, Keatinge-Clay AT. How cis-acyltransferase assembly-line ketosynthases gatekeep for processed polyketide intermediates. ACS Chem Biol. 2021;16(11):2515–26.
89. Xue Y, Wilson D, Zhao L, Liu H, Sherman DH. Hydroxylation of macrolactones YC-17 and narbomycin is mediated by the pikC-encoded cytochrome P450 in *Streptomyces venezuelae*. Chem Biol. 1998;5(11):661–7.
90. McCullough TM, Choudhary V, Akey DL, Skiba MA, Bernard SM, Kittendorf JD, et al. Substrate trapping in polyketide synthase thioesterase domains: structural basis for macrolactone formation. BioRxiv. 2024;294:421.
91. Hong JS, Park SH, Choi CY, Sohng JK, Yoon YJ. New olivosyl derivatives of methymycin/pikromycin from an engineered strain of *Streptomyces venezuelae*. FEMS Microbiol Lett. 2004;238(2):391–9.
92. Burger MT, Hiebert C, Seid M, Chu DT, Barker L, Langhorne M, et al. Synthesis and antibacterial activity of novel C12 ethyl ketolides. Bioorg Med Chem. 2006;14(16):5592–604.
93. Mahama O, Songuigama C. Pharmacochemical aspects of the evolution from erythromycin to neomacrolides, ketolides and neoketolides. Open J Med Chem. 2020;10(3):57–112.
94. Hagen A, Poust S, de Rond T, Yuzawa S, Katz L, Adams PD, et al. In vitro analysis of carboxyacyl substrate tolerance in the loading and first extension modules of borrelidin polyketide synthase. Biochemistry. 2014;53(38):5975–7.

95. Lowden PA, Bohm GA, Metcalfe S, Staunton J, Leadlay PF. New rapamycin derivatives by precursor-directed biosynthesis. ChemBioChem. 2004;5(4):535–8.
96. Pickar-Oliver A, Gersbach CA. The next generation of CRISPR-Cas technologies and applications. Nat Rev Mol Cell Biol. 2019;20(8):490–507.
97. Slaymaker IM, Gao L, Zetsche B, Scott DA, Yan WX, Zhang F. Rationally engineered Cas9 nucleases with improved specificity. Science. 2016;351(6268):84–8.
98. Kleinstiver BP, Pattanayak V, Prew MS, Tsai SQ, Nguyen NT, Zheng Z, et al. High-fidelity CRISPR-Cas9 nucleases with no detectable genome-wide off-target effects. Nature. 2016;529(7587):490–5.
99. Kuhstoss S, Rao RN. A thiostrepton-inducible expression vector for use in Streptomyces spp. Gene. 1991;103(1):97–9.
100. Rodriguez-Garcia A, Combes P, Perez-Redondo R, Smith MC, Smith MC. Natural and synthetic tetracycline-inducible promoters for use in the antibiotic-producing bacteria Streptomyces. Nucleic Acids Res. 2005;33(9): e87.
101. Wang W, Yang T, Li Y, Li S, Yin S, Styles K, et al. Development of a synthetic oxytetracycline-inducible expression system for streptomycetes using de novo characterized genetic parts. ACS Synth Biol. 2016;5(7):765–73.
102. Noguchi Y, Kashiwagi N, Uzura A, Ogino C, Kondo A, Ikeda H, et al. Development of a strictly regulated xylose-induced expression system in Streptomyces. Microb Cell Fact. 2018;17(1):151.
103. Yang Q, Luan M, Wang M, Zhang Y, Liu G, Niu G. Characterizing and engineering rhamnose-inducible regulatory systems for dynamic control of metabolic pathways in streptomyces. ACS Synth Biol. 2024;13(10):3461–70.
104. Wang X, Fu Y, Wang M, Niu G. Synthetic cellobiose-inducible regulatory systems allow tight and dynamic controls of gene expression in streptomyces. ACS Synth Biol. 2021;10(8):1956–65.
105. Bai C, van Wezel GP. CUBIC: a versatile cumate-based inducible CRISPRi system in streptomyces. ACS Synth Biol. 2023;12(10):3143–7.
106. Horbal L, Fedorenko V, Luzhetskyy A. Novel and tightly regulated resorcinol and cumate-inducible expression systems for Streptomyces and other actinobacteria. Appl Microbiol Biotechnol. 2014;98(20):8641–55.
107. Herai S, Hashimoto Y, Higashibata H, Maseda H, Ikeda H, Omura S, et al. Hyper-inducible expression system for streptomycetes. Proc Natl Acad Sci U S A. 2004;101(39):14031–5.
108. Murakami T, Holt TG, Thompson CJ. Thiostrepton-induced gene expression in *Streptomyces lividans*. J Bacteriol. 1989;171(3):1459–66.
109. Lim JH, Lee CR, Dhakshnamoorthy V, Park JS, Hong SK. Molecular characterization of Streptomyces coelicolor A(3) SCO6548 as a cellulose 1,4-beta-cellobiosidase. FEMS Microbiol Lett. 2016. https://doi.org/10.1093/femsle/fnv245.
110. Kurosawa K, Wewetzer SJ, Sinskey AJ. Engineering xylose metabolism in triacylglycerol-producing *Rhodococcus opacus* for lignocellulosic fuel production. Biotechnol Biofuels. 2013;6(1):134.
111. Pasquier E, Viguie C, Fini JB, Mhaouty-Kodja S, Michel-Caillet C. Limits of the regulatory evaluation of resorcinol as a thyroid disruptor: when limited experimental data challenge established effects in humans. Environ Res. 2023;222: 115330.
112. Krysenko S. Current approaches for genetic manipulation of Streptomyces spp.-key bacteria for biotechnology and environment. BioTech (Basel). 2025;14(1):3.

Publisher's Note